Article scientifique   Article   1992   **Published version**   Open Access

This is the published version of the publication, made available in accordance with the publisher's policy.

Dynamic global-to-direct irradiance conversion models

Ineichen, Pierre; Perez, R.R; Seal, R.D; Maxwell, E.L; Zalenka, A

DYNAMIC GLOBAL-TO-DIRECT IRRADIANCE CONVERSION MODELS

R.R. Perez, Ph.D.
Member ASHRAE

P. Ineichen, Ph.D.

E.L. Maxwell, Ph.D.

R.D. Seals

A. Zelenka, Ph.D.

ABSTRACT

This paper presents two models for converting hourly global into hourly direct beam irradiance based on a new parameterization of insolation conditions (Perez et al. 1990a). This parameterization does not require any additional input data than those already contained in a global irradiance time series but attempts to better utilize available information. The models are capable of using surface dew-point temperature as an additional input when this is available.

The models are derived statistically from a large multiclimatic experimental data base. The two models differ technically but should be functionally equivalent: The first is a correction to the physically based DISC model (Maxwell 1987); the second consists of a set of simple linear relationships.

Validation results are presented in reference to three existing models (Maxwell 1987; Erbs et al. 1982; Randall and Whitson 1977). The validation benchmarks consist of root mean square and mean bias errors as well as the ability of the models to recreate the skewness and kurtosis of actual direct irradiance distributions.

INTRODUCTION

Knowing the direct and diffuse components of global solar radiation is important for solar-related applications, since each affects systems in fundamentally different ways. Moreover, the two components are critical inputs for conversion models, such as the calculation of irradiance impinging on a tilt (Kondratyev 1969; Hay and Davies 1980; Perez et al. 1989).

Recently developed instruments (Michalsky et al. 1986; Kern 1990) will make the measurement of these components both practical and affordable on a large scale. Unfortunately, most of the existing long-term irradiance data bases only contain global measurements. Therefore, adequate models that extrapolate the two components from the global values are needed to exploit these data bases properly.

Since the original Liu and Jordan (1960) correlations, model precision has steadily improved. At the hourly level, note the well-known Orgill and Hollands (1977) and Erbs et al. (1982) correlations selected as best performers by the International Energy Agency (IEA) (Davies et al. 1988). More recently, note the model by Skartveit and Olseth (1987) and Maxwell's (1987) DISC model. Finally, note the updated correlations by Reindl et al. (1989) published during the course of this work.

We recently evaluated the DISC, the Skartveit and Olseth, and the Erbs models (Perez et al. 1990b). The DISC model was found to perform best overall. However, we noted that performance improvements were possible without additional input because of the systematic bias patterns observed with each model.

METHODS

A model may be regarded as a transfer function between a set of inputs and a desired output. Most often, the limiting factor in the utility of a model is not the complexity of its transfer function but the availability and interpretation of the input information fed to the model. Hence, the notion of insolation condition parameterization is a key consideration.

Parameterization of Insolation Conditions

The insolation conditions are parameterized as a multidimensional space. Each dimension is a direct function of the sky condition information at hand.

The first two dimensions are based on information that is always available with a given hourly global irradiance record: global irradiance itself plus the record's time and location. The two corresponding dimensions are the solar zenith angle Z and the clearness index Kt'. Here, we use a zenith angle-independent expression of the clearness index, based on Kasten's (1980) pyrheliometric formula, that we previously proposed (Perez et al. 1990a)

$$Kt' = Kt/(1.031 \cdot \exp(-1.4/(0.9 + 9.4/m)) + 0.1), \quad (1)$$

where Kt is the ratio of global to extraterrestrial irradiance on a horizontal plane and m is the air mass from Kasten (1966). This expression ensures that a given Kt', unlike the classic index Kt, will represent meteorologically similar conditions regardless of the sun's position.

The third dimension is available anytime global irradiance is available as a time series, which is almost always the case. We recently proposed a "stability index" $\Delta Kt'$ (Perez et al. 1990a) that accounts for the dynamics of the time series. It is defined by

$$\Delta Kt' = 0.5 \cdot (|Kt'_i - Kt'_{i+1}| + |Kt'_i - Kt'_{i-1}|), \tag{2}$$

where the subscripts i, $i+1$, and $i-1$ refer, respectively, to the current, the next, and the previous hourly record. If either the preceding or following hourly record is missing (e.g., beginning or end of day), $\Delta Kt'$ may be expressed as

$$\Delta Kt' = |Kt'_i - Kt'_{i\pm1}|. \tag{3}$$

For a given clearness level, stable conditions will be characterized by low $\Delta Kt'$ values and unstable conditions by high $\Delta Kt'$ values. This distinction makes it possible, for instance, to differentiate between hazy and partly cloudy conditions for a given value of Kt'.

Note that a similar stability index was derived independently by Skartveit and Olseth (1989) for the purpose of modeling the short-term variations of irradiance. Also note the work by Jeter et al. (1990), who proposed a stability index based on the standard deviation of global irradiance within a given hourly record; unfortunately, the needed input would generally not be available with historical data sets.

Other independent dimensions may be added if additional information relevant to direct irradiance transmission is known. For the present study, we selected the surface dew-point temperature Td. This measurement is routinely available and typically exhibits small time or space gradients; hence data from a neighboring weather station may be used safely. In addition, Td is an adequate estimator of atmospheric precipitable water (e.g., see Garrison and Adler [1990] and Wright et al. [1988]), which strongly influences absorption (hence direct vs. diffuse) as well as aerosol growth (hence scattering and direct-to-diffuse ratio). The corresponding fourth dimension is the atmospheric precipitable water W, estimated from surface dew-point temperature in °C from Wright et al. (1988):

$$W = \exp(0.07 \cdot Td - 0.075). \tag{4}$$

In summary, the four insolation condition dimensions are (1) the solar zenith angle Z, (2) the clearness index Kt', (3) the stability index $\Delta Kt'$, and (4) the precipitable water W.

The models presented hereafter are designed to use up to four dimensions but automatically revert to three or even two dimensions depending on the available input. For the present study, we will mainly refer to two operational modes: (1) a "3-D" mode, using only the input available within a global irradiance time series, and (2) a "4-D" mode, making use of surface dew-point temperature whenever available.

Modeling Approach

The models are derived statistically from a large multiclimatic experimental data set described below. This empirical approach is justified by our parameterization choice (which does not lend itself well to a first-principles physical derivation) and because achieving all-weather accuracy with a physical model would require considerably more detailed input data that is not generally available.

We use a multidimensional binning of the insolation condition space as a support for the models. The binning process ensures that each dimension is treated independently (unlike, for instance, stepwise regression). This approach results in a model that consists of a multidimensional "look-up" table plus a simple mathematical support. This structure will make any future code revisions straightforward. Such a code revision may be prompted by the availability of a larger pool of quality experimental data.

Although the binning process results in a large number of "coefficients," it has definite computational efficiency benefits. In fact, the model's look-up table is the digitized form of a complex, multidimensional analytical expression requiring considerably more CPU time. To further deflect concerns about our utilization of multicoefficient tables, note that when the present models are used and access a given coefficient in the look-up table, this coefficient is, on average, the statistical product of 500 experimental data points if the model is used in the 3-D mode and 65 data points when used in the 4-D mode. Finally, note that coefficients were not derived if less than five experimental events were found in a given bin but were extrapolated from neighboring bins.

Two Models We began our investigation with the goal of deriving an insolation-dependent correction for the quasi-physical DISC model (Maxwell 1987). However, recognizing the fact that the key element to the problem is the parameterization of insolation conditions, we also propose a simple mathematical support to go directly from global to direct irradiance.

The first model consists of the Solar Energy Research Institute's DISC model modified by an insolation-dependent factor. Direct irradiance I is obtained from

$$I = I_{disc} \cdot X(Kt', Z, W, \Delta Kt'), \tag{5}$$

where I_{disc} is the direct normal irradiance estimated by the DISC model (itself a function of global irradiance and solar zenith angle) and $X(Kt', Z, W, \Delta Kt')$ is a coefficient function of the four insolation condition parameters. This

coefficient is obtained from a four-dimensional look-up table consisting of a $6\times6\times5\times7$ matrix based on the bins in Table 1.

In the second model, direct irradiance I is obtained from

$$I = I_o \cdot Kb'$$
$$\cdot \exp(-1.4/(0.9 + 9.4/m))/0.87291, \qquad (6)$$

where I_o is the normal incident extraterrestrial irradiance, m is the air mass, and Kb' is a solar position-independent direct transmittance index based on Kasten's (1980) pyrheliometric formula. Kb' is obtained from

$$Kb' = 0 \text{ if } Kt' < 0.2,$$
$$\text{otherwise}$$
$$Kb' = a(Kt', Z, W, \Delta Kt') \cdot Kt'$$
$$+ b(Kt', Z, W, \Delta Kt'),$$

where the terms a and b are obtained from four-dimensional look-up tables consisting of $8\times5\times4\times6$ matrices based on the bins in Table 1. The bins were selected so that the observed rate of change of Kb' vs. Kt' may be approximated to a constant within each bin.

Experimental Data

The coefficients for each model are derived via least-squares fitting of a large experimental data base. The two exceptions are:

TABLE 1

bins used for function $X(Kt', Z, W, \Delta Kt')$

Bin #	Kt' from	to	Z (°) from	to	W (cm) from	to	ΔKt' from	to
1	0.00	0.24	0	25	0	1	0.000	0.015
2	0.24	0.40	25	40	1	2	0.015	0.035
3	0.40	0.56	40	55	2	3	0.035	0.070
4	0.56	0.70	55	70	3	∞	0.070	0.150
5	0.70	0.80	70	80	0	∞ ^	0.150	0.300
6	0.80	1.00*	80	90**			0.300	1.000*
7							0.000	1.000^

bins used for $a(Kt', Z, W, \Delta Kt')$ and $b(Kt', Z, W, \Delta Kt')$

Bin #	Kt' from	to	Z (°) from	to	W (cm) from	to	ΔKt' from	to
1	0.00	0.29	0.0	40.0	0.00	1.50	0.000	0.020
2	0.29	0.42	40.0	52.5	1.50	2.75	0.020	0.048
3	0.42	0.53	52.5	65.0	2.75	∞	0.048	0.110
4	0.53	0.64	65.0	75.0	0.00	∞ ^	0.110	0.250
5	0.64	0.71	75.0	90.0**			0.250	1.000*
6	0.71	0.75					0.000	1.000^
7	0.75	0.79						
8	0.79	1.00*						

* Values of Kt' above 0.87 should be considered suspect for sites below 1000 m elevation.
** The model was validated only for Z < 85°. Utilization above this level should be done with caution.
^ Note that the highest W and Δkt' bins incorporate all bins; they are used respectively when W and Δkt' are not available (3-D and 2-D model modes).

1. for the modified DISC model, coefficients are not derived experimentally if less than five events are found in a given bin but extrapolated from more populated neighboring bins;
2. for the linear model, the experimental data set is complemented with a synthetic set, similar in size, generated with the modified DISC model. Since the linear model does not have a physically based support, a straightforward fitting process could lead to considerable distortion in unevenly or low populated bins. In order to avert this potential shortcoming, we complemented the experimental data base with synthetic data from the first model. The process ensures that the simple model retains a physical basis and that its performance is comparable to that of the corrected DISC model.

The data base contains more than 58,000 records from 18 measurement stations at 15 sites in North America and Europe. Climatic environments cover a wide range from marine temperate to arid, including subtropical, high elevation, and polluted environments. As a consequence, a model derived from the ensemble of the data should have minimal site dependency. The climatic environment of each data set is briefly described in Table 2. The table also indicates whether or not dew-point temperature was available for this study.

The set consists mainly of research data, where close supervision was given to day-to-day acquisition and calibration monitoring and where data were subjected to stringent on-site quality control. Only four of the sites are from a solar monitoring network (Maxwell 1988). They were selected after having undergone in-depth post-measurement quality control at SERI (1990). WMO class I radiometric instruments were used at each site.

The different measurement practices, instrumentation types and calibration sources, and methodologies at each site should be an asset to the models rather than a liability. Indeed, such diversity contributes to model universality, since this will not be dependent on the idiosyncrasies found at a particular site. The only common denominator to all the data bases is the normal incidence pyrheliometer used to measure direct irradiance—as a consequence, the present model's performance is linked to the instrument's accuracy.

Model Validation

Model performance is evaluated individually against each site's data using four validation benchmarks. The first two are standard model validation measures quantifying a model's long-term and short-term performance. These are

1. the model's mean bias error (MBE),

$$\text{MBE} = [\Sigma_i(\text{model}_i - \text{truth}_i)]/(n-1), \qquad (8)$$

where n is the number of data points and i denotes a given event, and

2. the model's root mean square error (RMSE),

$$\text{RMSE} = \{[\Sigma_i(\text{model}_i - \text{truth}_i)^2]/(n-1)\}^{0.5}. \quad (9)$$

The other two benchmarks represent the model's ability to recreate key statistical characteristics of actual irradiance distributions, namely, their skewness and kurtosis, which quantify, respectively, the distribution's asymmetry and peakedness. The benchmarks are

3. modeled minus actual skewness S, where

$$S = \mu_3/\mu_2^{3/2}, \quad (10)$$

where μ_2 and μ_3 are the second and third moments of the direct irradiance distribution, and

4. modeled minus actual kurtosis K, where

$$K = \mu_4/\mu_2^2, \quad (11)$$

where μ_4 is the fourth moment of the distribution.

Test Dependency The experimental data sets used for model development are also used for validation. Hence, one may advance that validation is not dependent. This argument may be refuted on two grounds. First the data base is very diverse and encompasses a wide spectrum of climatic environments and measurement particularities, practically eliminating any site specificity. Second, genuinely independent tests were performed for each site using versions of the model developed from all but the test site's data. The resulting RMSE degradation was found to range from less than 1 W/m^2 for more than half the sites to 3 to 4 W/m^2 for the two sites with the most different environmental characteristics.

TABLE 2

Site	Climate/Environment Main Features	Data Set Span	Td Available
Geneva, Switzerland (Ineichen 1988)	Temperate maritime, with central Europe continental influence.	1 year	Yes
Cabauw, Netherlands (VandenBrink 1984)	Northern Europe temperate maritime	1 year	No
Trappes, France (ONM; U.S. DOE)	Temperate maritime	1 year	No
Carpentras, France (ONM; U.S. DOE)	Mediterranean	1 year	No
Albany, NY, USA (N.Y. State)	Humid continental (2 independent data sets)	1 year + 1 year	Yes No
New York, NY, USA (N.Y. State)	Same with maritime influence plus large city's environment	1 year	Yes
Farmingdale, NY, USA (N.Y. State)	Same as above but without city's environment	1 year	Yes
Oswego, NY, USA (N.Y. State)	Humid continental, Great Lakes basin	6 months	Yes
Glens Falls, NY, USA (N.Y. State)	Humid continental, Adirondack Mountains	6 months	Yes
Phoenix, AZ, USA (U.S. DOE)	Arid, low elevation	6 months	Yes
Albuquerque, NM, USA (U.S. DOE)	Arid, High elevation (2 independent data sets)	1 year + 2 years	No No
Los Angeles, CA, USA (U.S. DOE)	Arid + maritime influence + smog (2 independent data sets)	6 months + 1 year	Yes No
C. Canaveral, FL, USA (Fla. Solar)	Subtropical, low latitude, maritime	1.5 year	Yes
Brownsville, TX USA (TMY)	Same with higher cloudiness and more continental influence	2 years	No
Bismarck, ND USA (TMY)	Dry Continental plus extensive winter-time snow cover	1.5 year	No
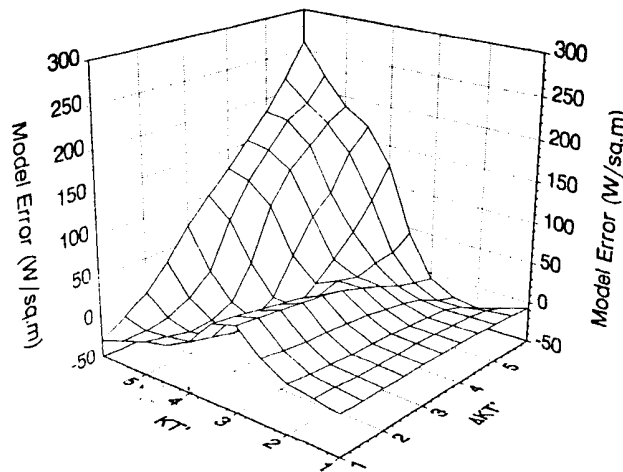
Figure 1 Original DISC model error as a function of clearness (Kt') and stability (ΔKt') indices.

RESULTS

Model Development

In this section, we briefly illustrate the role played by the new parameterization in delineating characteristics of global-to-direct conversion.

In Figure 1 is plotted the all-site mean bias error of the original DISC model as a function of clearness (Kt') and stability ($\Delta Kt'$). The resulting pattern is well defined and points out some limitations of this model. For high clearness conditions, the model goes from a slight underestimation of truth when conditions are stable to a large overestimation when conditions become unstable. This may be easily explained because high-clearness unstable conditions are likely representative of very thin, scattered cloud conditions keeping global irradiance at a high level but obstructing part of the direct irradiance (note that only the information contained in the global irradiance time series allows us to make this observation). Other features of Figure 1 show that the DISC model underestimates for unstable low-clearness conditions, probably because these are characterized by thick, slightly broken cloud decks letting some direct beam through. Finally, note the intermediate clearness overestimation "ridge" previously reported (Perez et al. 1990b). The modified DISC model incorporates the reciprocal of the bias pattern in Figure 1 as a correcting function.

Figures 2 and 3 illustrate the effects of the stability and precipitable water parameters on the relationship between direct transmittance (Kb') and clearness (Kt'). These plots were obtained by direct utilization of the simple algorithm (Equation 7).

Superimposed on the general S-shaped Kb'-Kt' relationship, the effect of stability discussed above is quite apparent. The influence of precipitable water is less marked but is well defined nonetheless. It is interesting to
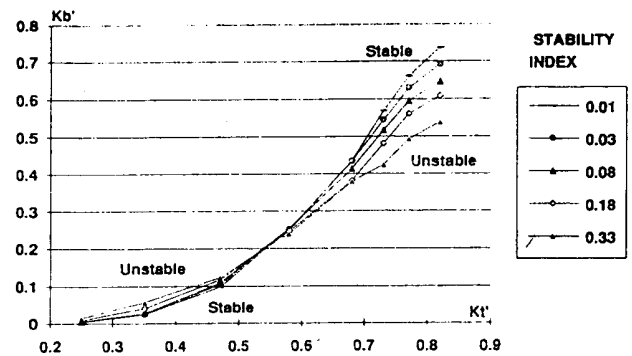
Figure 2 Effect of the stability index on the observed relationship between direct transmittance (Kb') and global transmittance (i.e., clearness index, Kt').
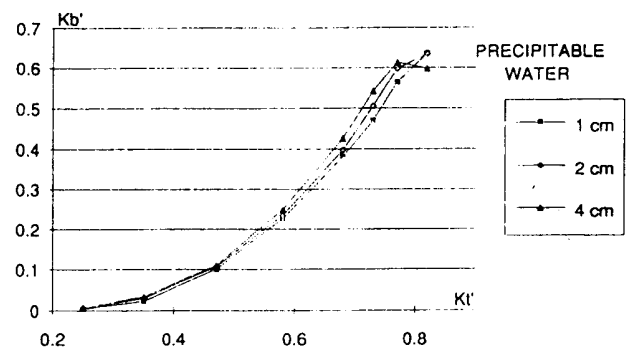
Figure 3 Effect of modeled atmospheric precipitable water on the observed relationship between direct transmittance (Kb') and global transmittance (Kt').

note that, for a given clearness index, there is more direct radiation available if conditions are humid than if they are dry, except for the highest clearness levels where the tendency is reversed. This observation, which is surprising at first (more water vapor would signify more long-wave absorption, hence less direct), is probably indicative of the fact that a given clearness index level is achieved by haze for humid conditions and by scattered clouds for dry conditions; the latter results in more direct beam obstruction and a brighter sky. When clouds are no longer present for very clear conditions, the driest cases logically result in the highest direct irradiance values.

Model Validation

The results presented below illustrate the performance of the modified DISC model in the 3-D and 4-D modes. The performance of the simple linear model is quite similar to that of the modified DISC with minor degradation in performance (1 to 2 W/m^2 increase in error).

Root Mean Square and Mean Bias Errors Validation results using the MBE and RMSE benchmarks are

TABLE 3

SITE	ETMY MBE	ETMY RMSE	ERBS MBE	ERBS RMSE	DISC MBE	DISC RMSE	3-D dKt' MBE	3-D dKt' RMSE	4-D Td MBE	4-D Td RMSE
Brownsville	-13	105	-20.9	94.4	-24.9	84.4	-28.8	80.6		
Cape Canaveral	-8	123	-31.6	110.5	-18.3	93.4	-22	86	-12.3	80.7
Albany 1	3	98.3	-19.4	90.1	-0.7	72.4	-7.4	64.7		
Albuquerque 1	23	113	-44	105	-3.8	79.5	-7.3	68		
Queens	1.7	93.8	-23.6	83	-0.9	69.5	-4.9	62.2	-10.5	62.2
Albuquerque 2	21	127.9	-43.8	114	5.1	86.8	-4.8	76		
Glens Falls	-11.6	100.5	-20.7	92.3	25.8	93.2	2.3	81.8	-9.8	79.1
Oswego	-10.8	99.1	-18.6	79.2	22.6	77.4	5.2	64.6	-4.9	58.1
Bismarck	11	124	-13.3	111.5	16.5	105.5	5.6	89.4		
Cabauw	-16.5	81	5.5	70	32	81.5	10.6	64.5		
Trappes	-18.5	83.6	3.5	72.3	24.1	74.5	14.1	61.9		
Albany 2	-15.3	93.7	-0.4	77.8	26.5	84.8	15.9	68.3	7.6	61.5
Farmingdale	-15.4	96.3	-4.8	77.5	24.7	72.7	17.7	64.1	9.6	60.2
Geneva	-20.8	94.4	6.3	87.4	30.9	86.9	21	70.4	11.3	62
Carpentras	6	100	-17.1	90.4	27	74.4	21.1	63.1		
Los Angeles 1	-28	122	-8.4	108.4	23	79.4	21.5	74.3		
Los Angeles 2	-12	114.5	-4.7	97.9	24.8	78.2	21.7	67.9	11.6	64.4
Phoenix	42.8	107.4	-24.5	93.5	21	81.4	22	69.4	5.9	59.7
Mean site (all sites)	-3	104	-16	92	14	82	6	71		
Mean site (Td sites)	-5	103	-14	89	17	82	9	71	1	65

MODEL MEAN BIAS AND RMS ERROR (W/sq.m)

summarized in Table 3. The performance of the 3-D and 4-D versions of the corrected DISC model is compared for each site to that of three reference models: (1) the original DISC model, (2) the Erbs et al. model (1982), and (3) the ETMY model developed by Randall et al. (1977). The ETMY was used to prepare the U.S. Typical Meteorological Year (TMY 1980) and WYEC data tapes (WYEC 1980).

Table 3 summarizes the gradual performance improvements from the ETMY to the present algorithm from more than 100 W/m^2 mean site RMSE to 65 W/m^2. Note that this improvement spans all climates studied. The 3-D algorithm results primarily in a reduction of RMSE compared to the DISC model, although mean bias errors are also reduced by an average of 5 W/m^2. Using dew-point temperature as an additional input results in an across-the-board reduction of remaining mean bias differences between high precipitable water sites, such as Cape Canaveral, and low precipitable water sites (which may be either dry warm or cool humid, e.g., Phoenix, Arizona, and Geneva, Switzerland).

As a final comment on Table 3, note that the validation results are, to a small extent, a function of the known quality of each data base. For instance, of the five New York State sites where the authors participated directly in data acquisition, the worst model performance occurred at the site where day-to-day quality control was the most difficult to achieve adequately.

Model performance using the RMSE and MBE benchmarks is further illustrated in Figures 4 through 11. For each model, we have selected a sample of environmentally distinct sites—New York, Phoenix, Cape Canaveral, Geneva, Bismarck, and Albuquerque—to visualize

performance as a function of insolation conditions and climate. Scatter plots of modeled vs. measured irradiance are provided in Figures 4 through 7 for the ETMY, the DISC, and the 3-D and 4-D models. These plots are further detailed in Figures 8 through 11, where model bias and root mean square errors have been plotted as a function of measured direct irradiance. The reduction in scatter from the ETMY to the DISC model is a result of the latter's effective use of air mass to calculate beam irradiance. A further noticeable reduction in scatter is observed at all sites from the DISC to the 3-D model: note that many of the overestimating outlying points, corresponding to unstable conditions, have been eliminated; this is particularly visible in Geneva, where intermediate and unstable conditions are frequent. Using the 4-D model results in an additional bias reduction that accounts for some of the remaining discrepancies between such diverse sites as Cape Canaveral, Phoenix, and Geneva.

Skewness and Kurtosis In Table 4, we report the direct irradiance distribution's skewness and kurtosis observed at each site. The relationship between these two statistical parameters and the site's environment is noteworthy. Skewness magnitude and sign are good indicators of a site's prevailing clearness. This is increasingly negative for the clearest sites in the southwestern U.S. and becomes increasingly positive for the cloudiest sites in northern New York and northern Europe; note that each site fits logically on the skewness scale as a function of its climate. Kurtosis reflects the extreme character of a climate as this increases for both the cloudiest and driest sites.

Model performance relative to these benchmarks is reported in Table 4, which includes the difference be-
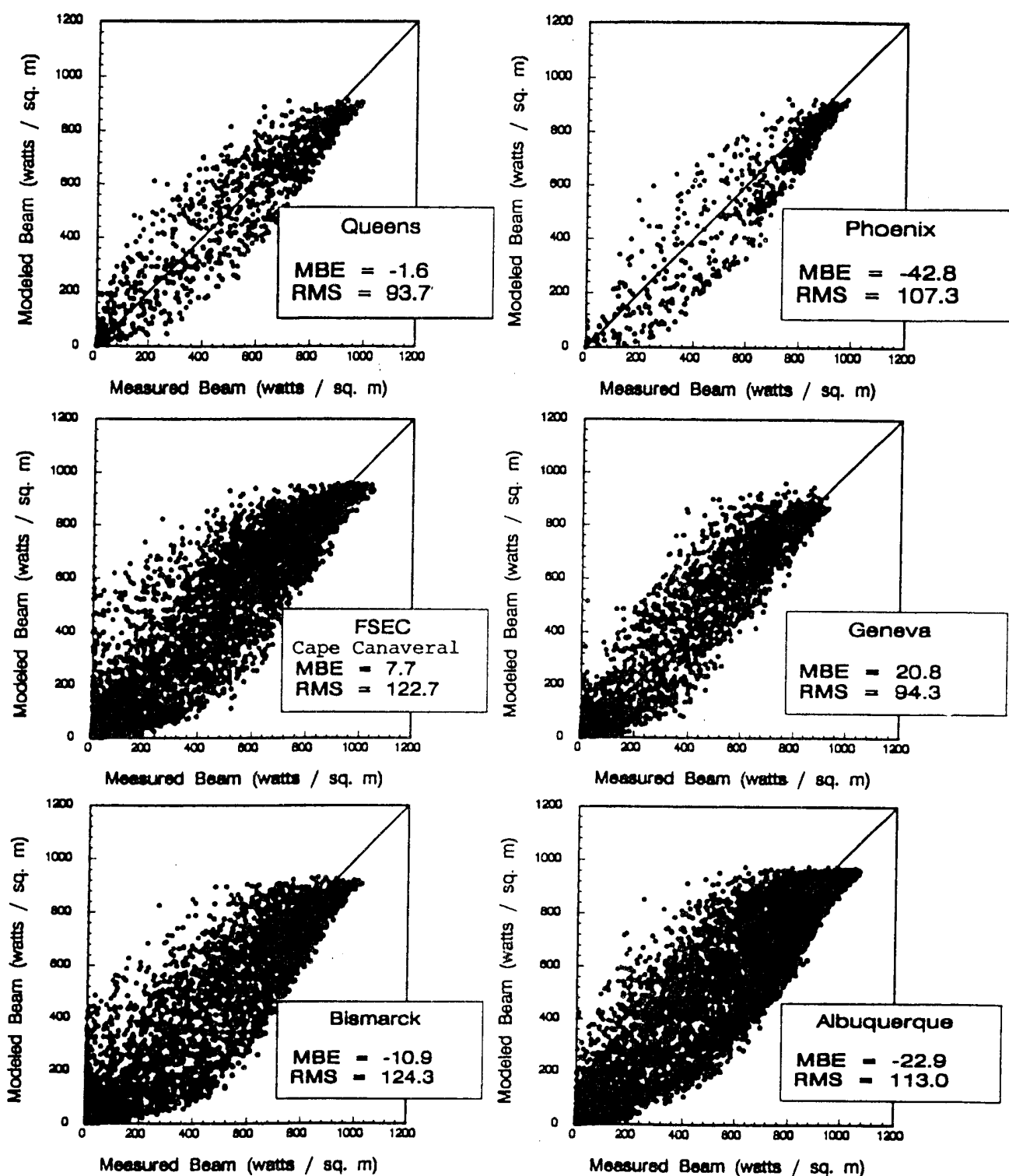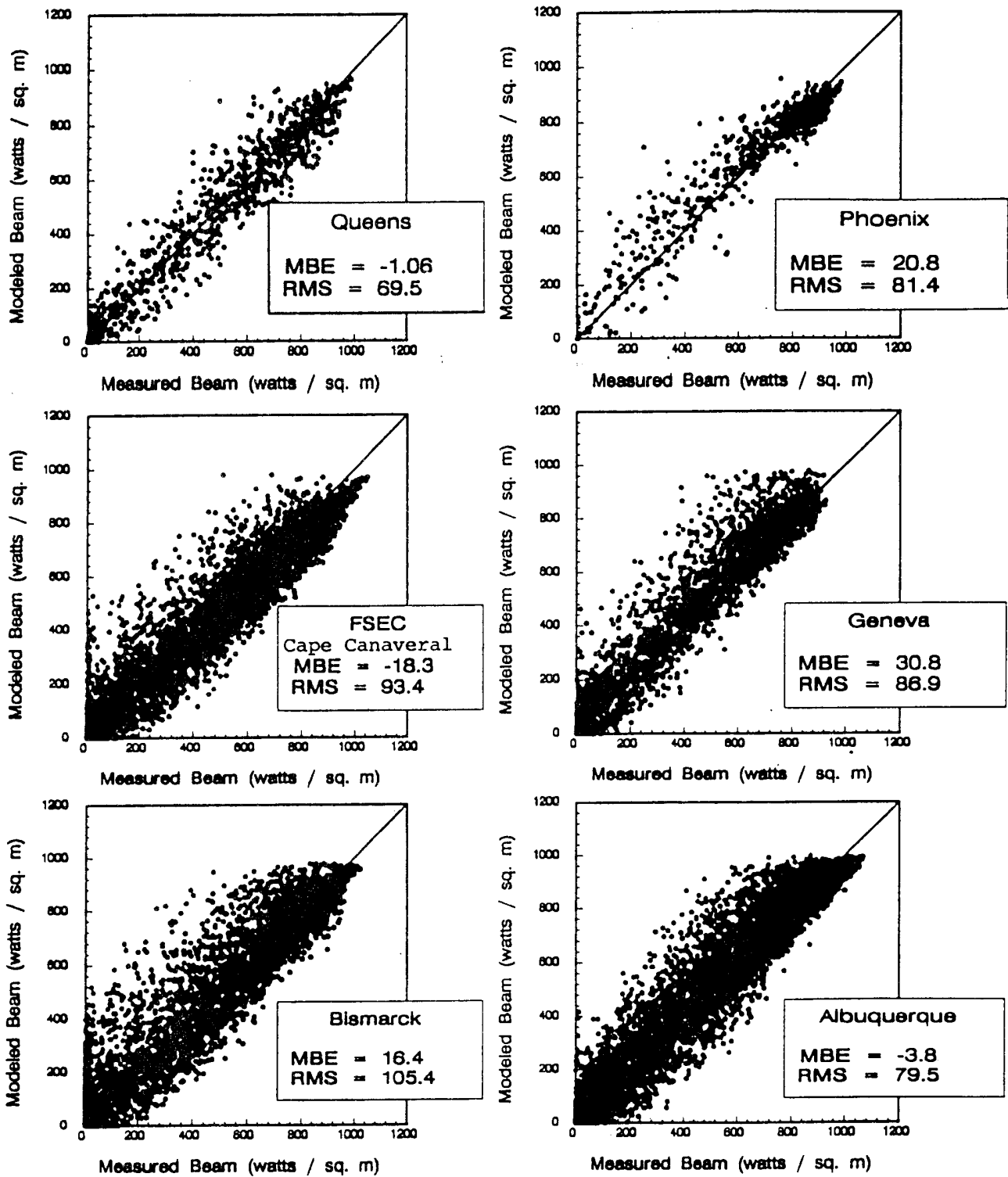
Figure 4   *Modeled vs. measured direct irradiance using the ETMY algorithm.*

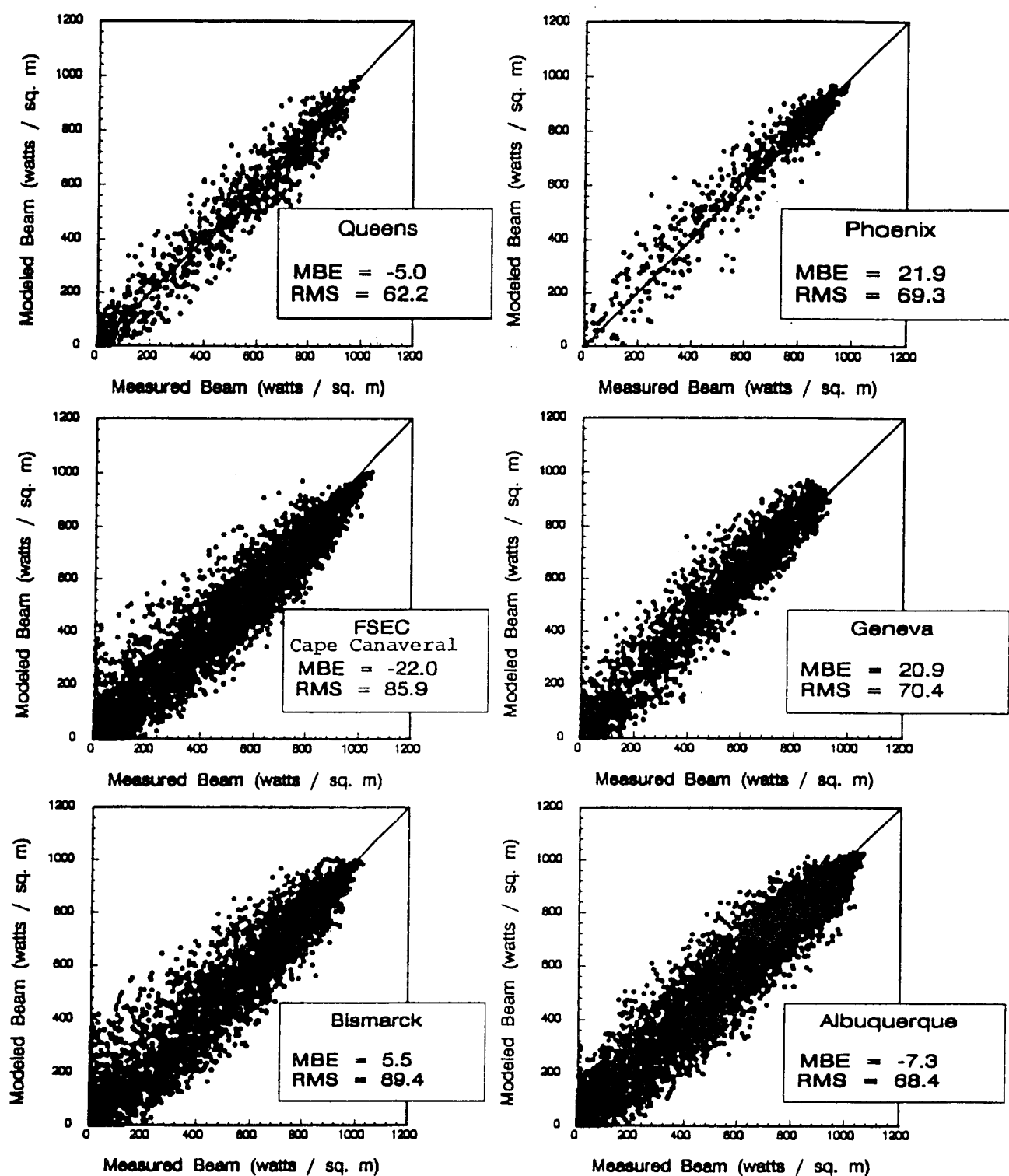*Figure 5*   *Modeled vs. measured direct irradiance using the DISC algorithm.*

Figure 6   *Modeled vs. measured direct irradiance*
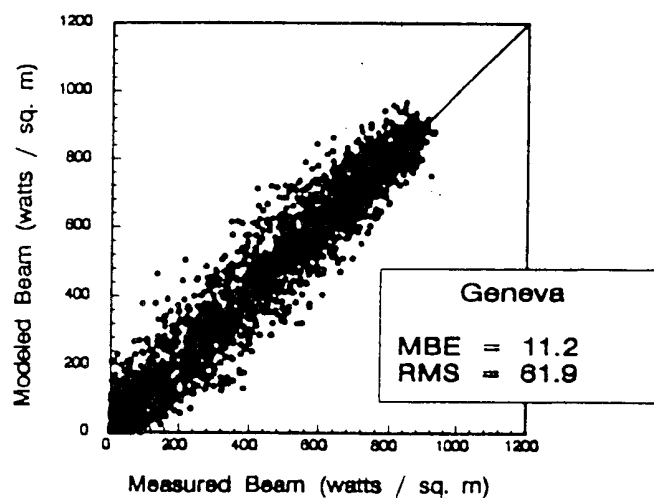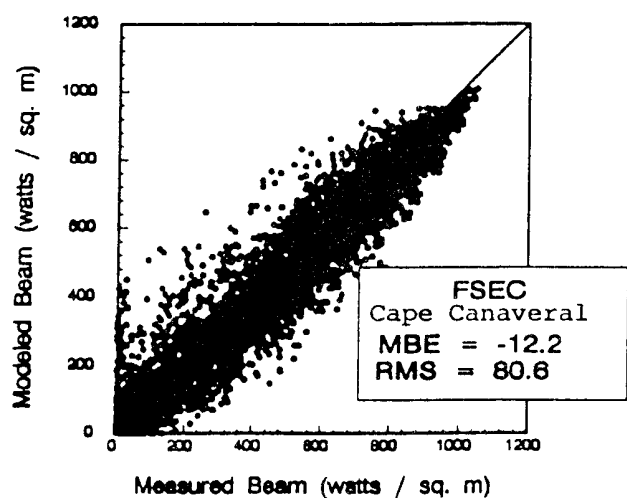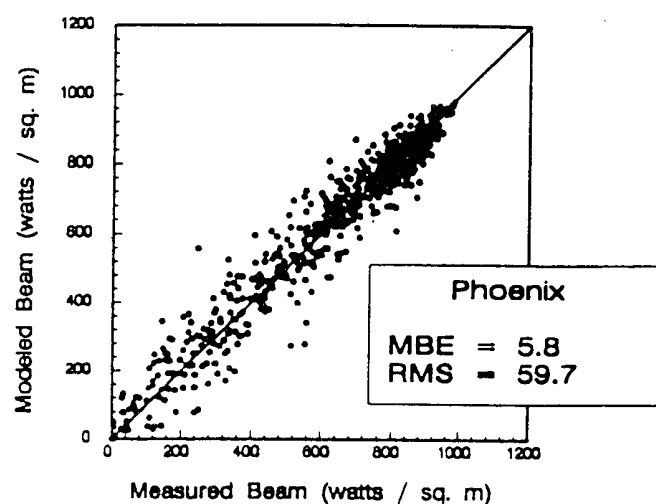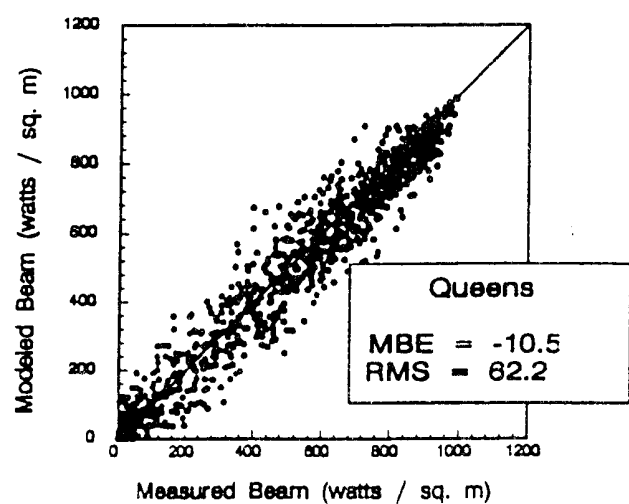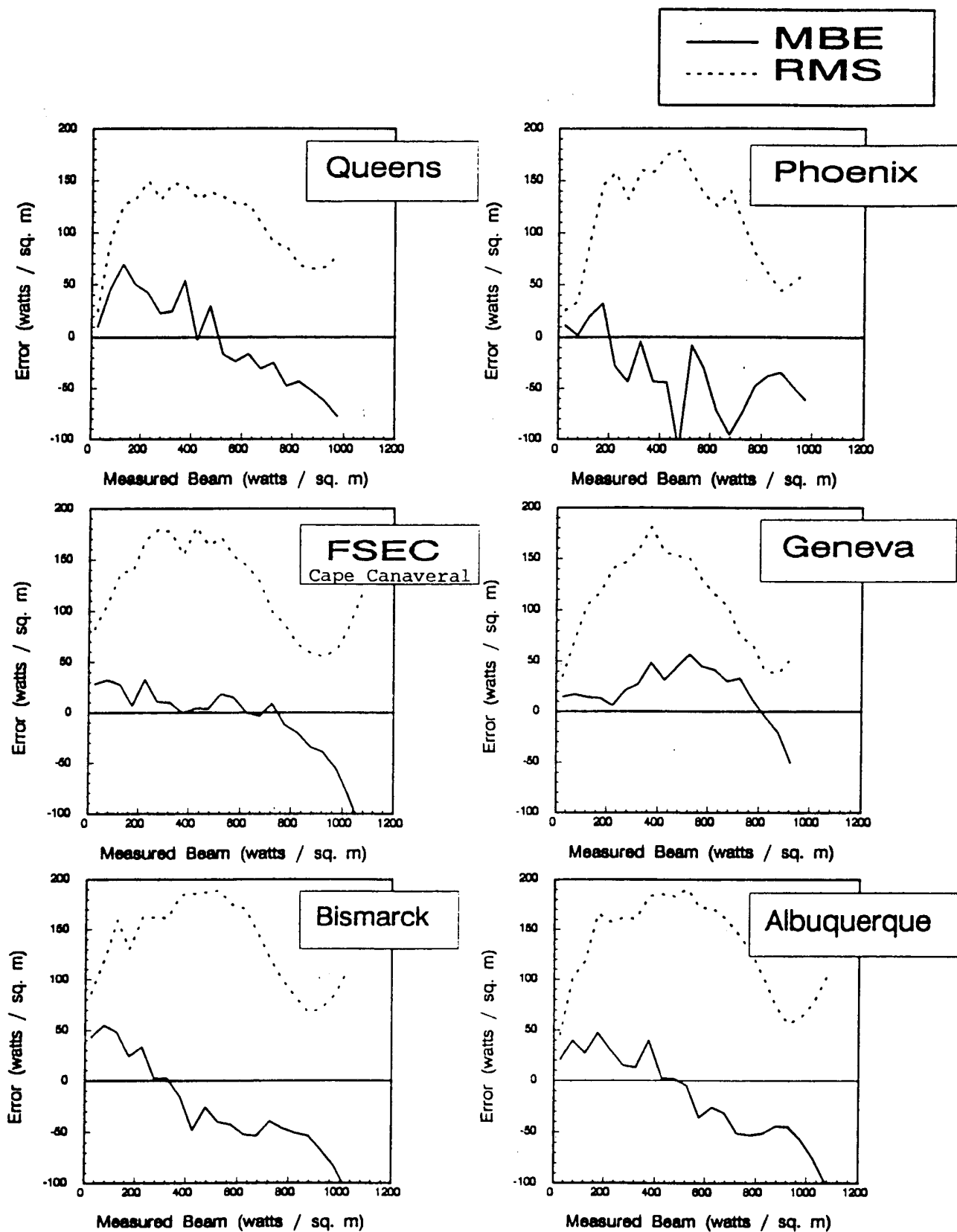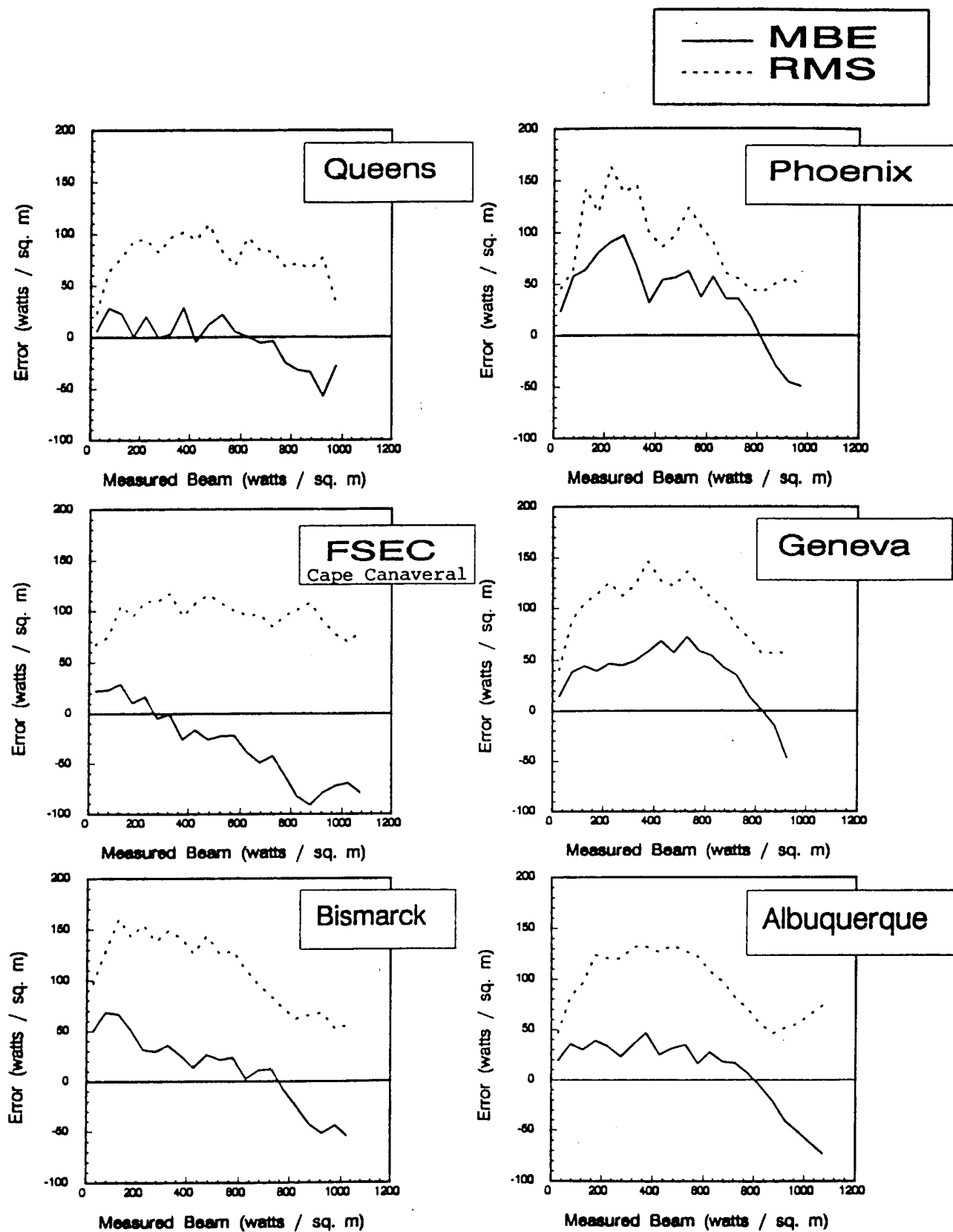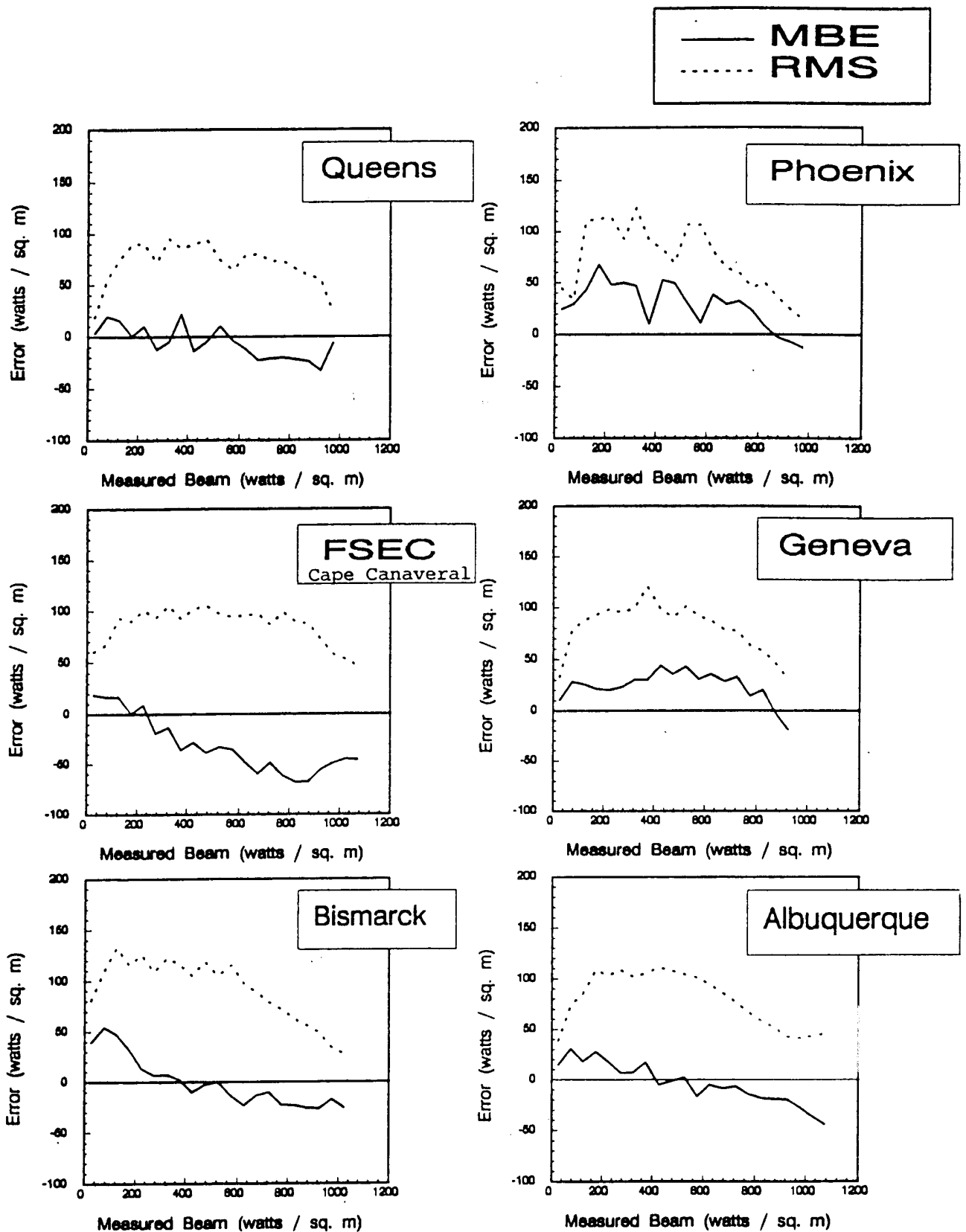*using the 3-D algorithm.*

Figure 7   *Modeled   vs.   measured   direct   irradiance*
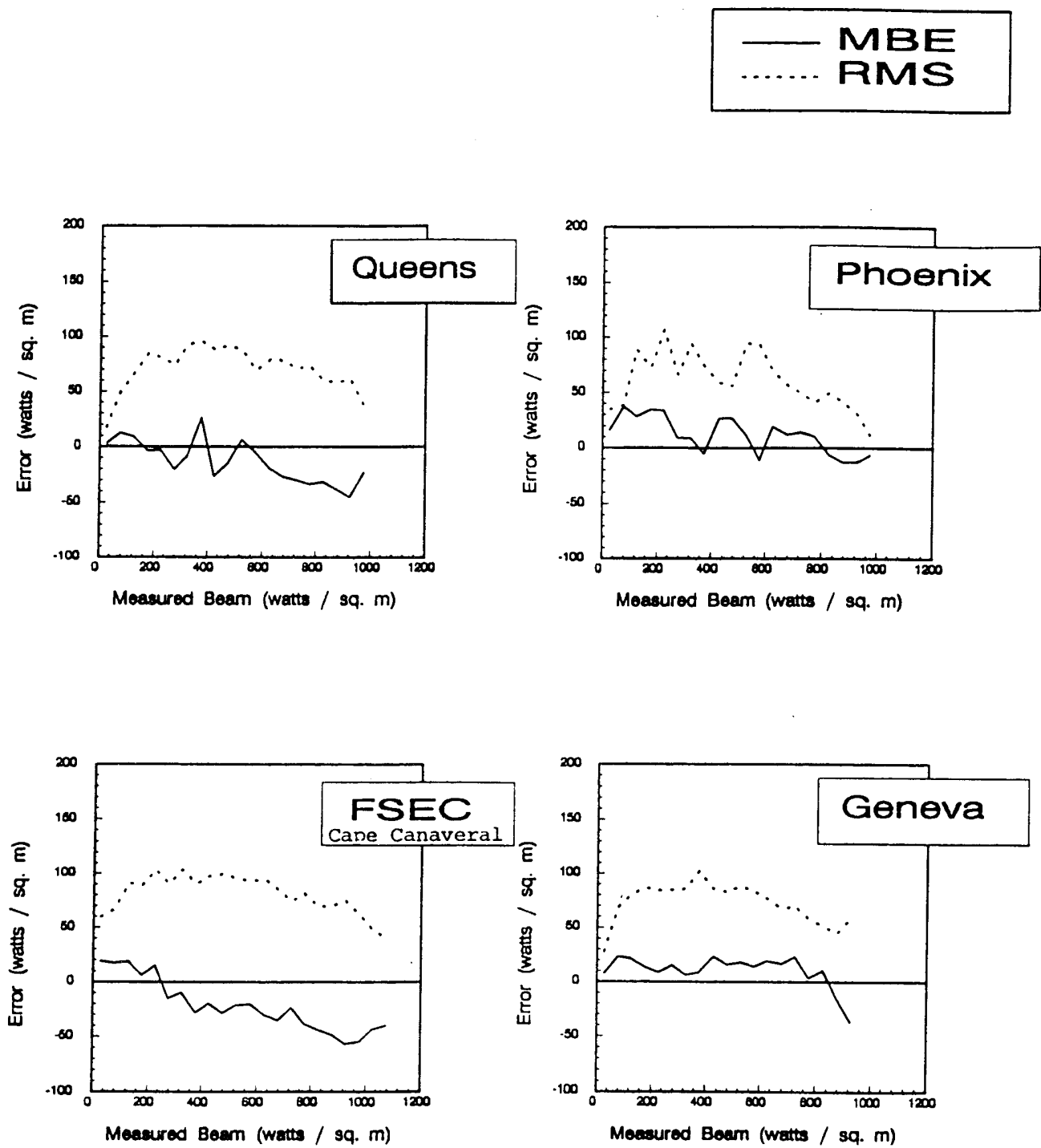*using the 4-D algorithm.*

Figure 8   *Model RMSE and MBE as a function of incoming direct irradiance for the ETMY algorithm.*

Figure 9   *Model RMSE and MBE as a function of incoming direct irradiance for the original DISC algorithm.*

Figure 10   *Model RMSE and MBE as a function of in-coming direct irradiance for the 3-D algo-rithm.*

Figure 11 *Model RMSE and MBE as a function of incoming direct irradiance for the 4-D algorithm.*

TABLE 4

	Skewness meas.	Model Error etmy	disc	3D	4D	Kurtosis meas.	Model Error etmy	disc	3D	4D
Phoenix, Arizona	-0.88	0.12	-0.29	-0.13	-0.05	2.68	-0.34	0.74	0.31	0.11
Albuquerque 1, New mexico	-0.59	0.00	-0.11	-0.01	NA	1.81	-0.03	0.11	0.02	NA
Albuquerque 2, New Mexico	-0.56	-0.03	-0.16	-0.04	NA	1.81	-0.01	0.19	0.07	NA
Los Angeles 1, California	-0.19	0.00	-0.06	0.00	NA	1.50	-0.07	0.06	0.06	NA
Carpentras, France	-0.17	0.02	-0.14	-0.06	NA	1.51	-0.10	-0.03	-0.02	NA
Los Angeles 2, California	-0.06	-0.01	-0.13	-0.08	-0.07	1.63	-0.15	0.05	0.04	0.03
Bismarck, N. Dakotta	-0.02	0.03	-0.07	0.00	NA	1.42	-0.02	0.04	0.06	NA
Cape Canaveral, Florida	0.09	-0.04	-0.03	0.03	0.01	1.55	-0.11	0.04	0.08	0.03
Queens, New York	0.19	-0.05	-0.02	0.01	0.00	1.49	-0.06	-0.02	0.02	0.00
Farmingdale, New York	0.37	-0.10	-0.10	-0.05	-0.05	1.54	-0.09	-0.12	-0.05	-0.06
Glens Falls, New York	0.34	-0.10	-0.10	-0.03	-0.02	1.57	-0.12	-0.09	0.00	0.00
Albany 1, New York	0.36	-0.09	-0.12	-0.06	-0.06	1.52	-0.13	-0.12	-0.05	-0.06
Brownsville, Texas	0.47	0.04	0.14	0.15	NA	1.86	-0.06	0.24	0.27	NA
Geneva, Switzerland	0.48	-0.02	-0.07	-0.03	-0.01	1.68	-0.11	-0.08	-0.04	-0.01
Albany 2, New York	0.61	-0.04	-0.04	0.01	NA	1.79	-0.06	-0.04	0.05	NA
Oswego, New York	0.79	-0.15	-0.14	-0.05	-0.03	2.11	-0.33	-0.21	-0.07	-0.03
Trappes, France	1.28	-0.13	-0.13	-0.07	NA	3.44	-0.51	-0.48	-0.24	NA
		Absolute Bias Error					Absolute Bias Error			
Mean site	0.15	0.06	0.11	0.05	0.03	1.82	0.14	0.16	0.09	0.04

tween modeled and measured values. It is interesting to note that the ETMY model scores better than the DISC model on these statistical grounds. Despite considerable shortcomings, the ETMY is "well balanced" overall and would provide a fair representativeness of a site's prevailing climate. The DISC model reduced much of the ETMY scatter but in an uneven fashion; the DISC model tends to underestimate skewness and to increase the kurtosis of clear sites and reduce that of cloudy sites. This is symptomatic of its tendency to systematically overestimate for high-clearness unstable cases (see Figure 5), in effect weighting the statistical distribution toward the high end. With a few minor exceptions, the 3-D model results in improved accuracy over the ETMY model. The 4-D model further reduces observed errors.

Model Availability and Utilization

The models are available as Fortran 77 functions with clearly specified input and output parameters. The source codes are available on 3.5-inch or 5.25-inch diskettes upon request to SERI or the ASRC for a minor processing fee.

They will be used at SERI for the production of revised WYEC and those TMY climatic data tapes where global irradiance was actually measured. These new data sets, which will also include daylight availability parameters, will be referred to as ASHRAE-WYEC2. SERI will be subsequently providing revised data sets for sites where global was not measured (Maxwell 1990).

The choice between the modified DISC and the simple model is left to the user; the former has a direct physical basis that many may prefer. Their performance was found to be comparable based on the present data set.

CONCLUSION

This paper has presented new algorithms to extrapolate hourly direct irradiance from global irradiance.

These algorithms were validated against a comprehensive multiclimatic set of data and demonstrated systematic improvement when compared to existing models. The gain in performance is due primarily to a better utilization of the information always available within a global irradiance time series, in particular its time dynamics. This parameterization proved helpful in accounting for some of the direct irradiance variability at constant clearness index; this may be particularly important for sites where intermediate sky conditions are frequent. Utilization of surface dew-point temperature as additional input data proved helpful in reducing remaining bias discrepancies between climatic extremes.

ACKNOWLEDGMENT

REFERENCES

Davies, J.A., D.C. McKay, G. Luciani, and M. Abdel-Wahab. 1988. Validation of models estimating solar radiation on horizontal surfaces. International Energy Agency, Solar Heating and Cooling Programme Task IX Final Report, IEA, Paris, France, and Solar Energy 44: 153-168.

Erbs, D.G., S.A. Klein, and J.A. Duffie. 1982. Estimation of the diffuse radiation fraction for hourly, daily and monthly average global radiation. Solar Energy 28: 293-302.

Garrison, J.D., and P. Adler. 1990. Estimation of precipitable water over the United States for application

to the division of solar radiation into its direct and diffuse components. *Solar Energy* 44: 225-241.

Hay, J.E., and J.A. Davies. 1980. Calculation of the solar radiation incident on an inclined surface. *Proc. First Canadian Solar Radiation Workshop*. Toronto, Ontario, Canada: Hay & Won.

Ineichen, P. 1988. Mesures de Rayonnement a Geneve (June 1986-May 1987). Groupe de Physique Appliquee, Universite de Geneve, Switzerland.

Jeter, S.M., and C.A. Balaras. 1990. Development of improved solar radiation models for predicting beam transmittance. *Solar Energy* 44: 149-156.

Kasten, F. 1980. A simple parameterization of the pyrheliometric formula for determining the Linke turbidity factor. *Meteorol. Rdsch* 33: 124-127.

Kasten, F., and A. Young. 1989. Revised optical air mass tables and approximation formula. *Applied Optics* 28(22): 4735-4738.

Kern, E. 1990. The southern New York network's rotating shadowband radiometer. Ascension Technology, Lincoln Center, MA (personal communication).

Kondratyev, K.Y. 1969. *Radiation in the atmosphere.* New York: Academic Press.

Liu, B.Y.H., and R.C. Jordan. 1960. The interrelationship and characteristic distribution of direct, diffuse and total solar radiation. *Solar Energy* 4: 1-19.

Maxwell, E.L. 1987. A quasi-physical model for converting hourly global to direct normal insolation. SERI/TR-215-3087. Solar Energy Research Institute, Golden, CO; and *Proc. Annual Meeting Amer. Solar Energy Soc.*, Portland, OR, July 12-16, pp. 35-46.

Maxwell, E.L. 1988. Current status of the NOAA SOLRAD network. *Solar Spectrum* 1(1) (newsletter of the American Solar Energy Society Resource Assessment Division, ASES, Boulder, CO).

Maxwell, E.L. 1990. Producing a 1961-1990 solar radiation data base for the United States. Proc. of ASES Annual Conference, Solar 1990, Austin, TX.

Michalsky, J.J., J.L. Berndt, and G.J. Schuster. 1986. A microprocessor-based rotating shadowband radiometer. *Solar Energy* 36: 465-470.

New York State Daylight Availability Resource Assessment Program (1986-1988). NYSERDA contract 724-CONBCS85. Albany, NY: Atmospheric Sciences Research Center.

ONM. Direction de la Meteorologie (1979-1981). Service Meteorologique Metropolitain, Stations #260 and #874. Paris, France: ONM.

Orgill, J.F., and K.G. Hollands. 1977. Correlation equation for hourly diffuse radiation on a horizontal surface. *Solar Energy* 19: 357-359.

Perez, R., P. Ineichen, R. Seals, J. Michalsky, and R. Stewart. 1989. Modeling daylight availability and irradiance components from direct and global irradiance. *Solar Energy* 44: 271-289.

Perez, R., P. Ineichen, R. Seals, and A. Zelenka. 1990a. Making full use of the clearness index for parameterizing insolation conditions. *Solar Energy* 45: 111-114.

Perez, R., R. Seals, A. Zelenka, and P. Ineichen. 1990b. Climatic evaluation of models that predict hourly direct irradiance from hourly global irradiance—Prospects for performance improvements. *Solar Energy* 44: 99-108.

Randall, C.M., and M.E. Whitson. 1977. Monthly insolation and meteorological data bases including improved direct insolation estimates. Report ATR-78(7592)-1. El Segundo, CA: Aerospace Corporation.

Reindl, D.T., W.A. Beckman, and J.A. Duffie. 1989. Diffuse fraction corrections. Proc. of ISES Biennal Meeting, Kobe, Japan, and *Solar Energy* 45: 1-8.

SERI. 1990. *User's manual for quality assessment of solar radiation data.* SERI Technical Report. Golden, CO: Solar Energy Research Institute.

Skartveit, A., and J.A. Olseth. 1987. A model for the diffuse fraction of hourly global radiation. *Solar Energy* 38: 271-274.

Skartveit, A., and J.A. Olseth. 1989. Internal presentation to International Energy Agency, Solar Heating and Cooling Program, Task IX meeting. IEA, Paris, France.

SNL. 1986. Sandia National Laboratories' measurement program for radiation modeling. Contract #56-5434. Albuquerque, NM: Sandia National Laboratories.

Solar radiation monitoring at the Florida Solar Energy Center, Cape Canaveral, FL.

Typical Meteorological Year (TMY) data tapes. 1980. Selected sites where global irradiance was measured and not modeled. Asheville, NC: DOC National Weather Service.

U.S. DOE's Solar Energy Meteorolocical Research and Training Sites Region II (1980-1982). Albany, NY: Atmospheric Sciences Research Center.

Van den Brink, G.J. 1984. Information on magnetic tapes with solar irradiance on inclined surfaces. Internal Note #303.226-1. Delft, the Netherlands: Technisch Physische Dienst.

Weather Year for Energy Calculations (WYEC) data tapes 1980. 51 sites in the U.S. and Canada. Atlanta: American Society of Heating, Refrigerating, and Air-Conditioning Engineers, Inc.

Wright, J., R. Perez, and J.J. Michalsky. 1988. Luminous efficacy of direct irradiance: Variations with insolation and moisture conditions. *Solar Energy* 42: 387-394.